

Temperature-dependent chemical and electronic structure of reconstructed GaAs (100) surfaces

I. M. Vitomirov, A. D. Raisanen, A. C. Finnefrock, R. E. Viturro, and L. J. Brillson
Xerox Webster Research Center, Webster, New York 14580

P. D. Kirchner, G. D. Pettit, and J. M. Woodall
IBM T. J. Watson Research Center, Yorktown Heights, New York 10598

(Received 22 February 1992; accepted 10 March 1992)

Low-energy electron diffraction, soft x-ray photoemission, cathodoluminescence (CL), and Auger electron spectroscopies have been performed to investigate the geometric, chemical, and electronic properties of GaAs (100) surfaces as a function of annealing temperature and surface reconstruction. These measurements indicate gradual changes in surface geometry, composition, deep level CL features, and Fermi-level (E_F) position with increasing temperature of surface preparation. In contrast, it was observed that pronounced changes in the surface ionization potential and work function between different surface reconstructions. For most of the desorption temperatures and surface reconstructions, the secondary electron emission exhibits characteristic double onsets, possibly due to the existence of differently reconstructed patches on the surface. The implications of these variations in the surface chemical and electronic structure of GaAs (100) surfaces on their metal contact properties. It was concluded that (a) unique characterization of these surfaces requires measurements of geometric ordering, chemical composition and bonding, and deep level emission in the band gap, and (b) the correlation of the surface geometry with chemical and electronic surface and interface structure points to the central role of surface preparation in achieving controlled Schottky barrier behavior.

I. INTRODUCTION

Schottky barriers continue to be a subject of intense research efforts and significant scientific controversy.¹⁻³ A new insight into the physical and chemical phenomena responsible for the electrostatic barrier formation was afforded by the use of molecular-beam epitaxy (MBE) as a technique for the growth of both semiconductor substrates and their metal contacts.^{4,5} This work established significant Schottky barrier height variations as a function of interface chemical composition and atomic ordering on MBE-grown GaAs (100), a result which is in sharp contrast to the "universal pinning" behavior commonly reported for contacts on the (110) cleavage face of melt-grown GaAs.^{4,5} A complete understanding of this discrepancy requires detailed electronic and structural *in situ* characterization of clean GaAs surfaces.⁶⁻⁸

Here we present studies of decapped GaAs (100) with a goal to establish the interdependence of surface geometric, chemical, and electronic properties over a full range of annealing temperatures (250–650 °C) and surface reconstructions. We have used high-resolution core level and valence band soft x-ray photoemission spectroscopy (SXPS) to monitor surface chemistry and Fermi-level (E_F) movement, and cathodoluminescence spectroscopy (CLS) to follow the energy distribution and relative emission intensities of surface and interface deep levels. Photoemission measurements indicate subtle but reproducible changes in the Ga 3d and As 3d core-level features with desorption temperature, in close agreement with previously published results.⁷ The relative intensity of these core-level emissions, indicative of surface composition, changes by a factor of two between the As-rich and Ga-rich reconstructions,

in accord with the previous work of Bachrach *et al.*⁹ The surface E_F position is typically ~0.6 eV above the valence band maximum (E_v) throughout the temperature range of the $c(8\times 2)$ reconstruction. This relative insensitivity of the E_F position to surface composition is corroborated by the CL results which show only minor variations in deep level (DL) emission at clean surfaces prepared similarly.^{6,8} In contrast, we observe large (0.5–1.1 eV) changes in the surface ionization potential and work function between different surface reconstructions. We also find evidence of surface inhomogeneity in the appearance of characteristic double onsets in secondary electron emission from these thermally processed surfaces. Such inhomogeneity is likely due to the existence of surface patches with different reconstructions.¹⁰ We conclude that surface electronic states of decapped GaAs (100) surfaces are highly sensitive to surface bonding and composition, which can also play a major role in the Schottky barrier evolution at these surfaces.

II. EXPERIMENTAL DESCRIPTION

High-resolution SXPS experiments were conducted at the University of Wisconsin Aladdin storage ring using the Grasshopper Mark II and 6 m toroidal grating (TGM) monochromator and beamline. Valence-band spectra and both the surface- and more bulk-sensitive Ga 3d and As 3d energy distribution curves (EDCs) were acquired for clean and metallized surfaces. These spectra were subsequently analyzed using a least-squares line shape fitting routine in order to separate chemistry-related and electrostatic changes in core-level binding energies.¹¹ Photoemission determination of the surface ionization potential was carried

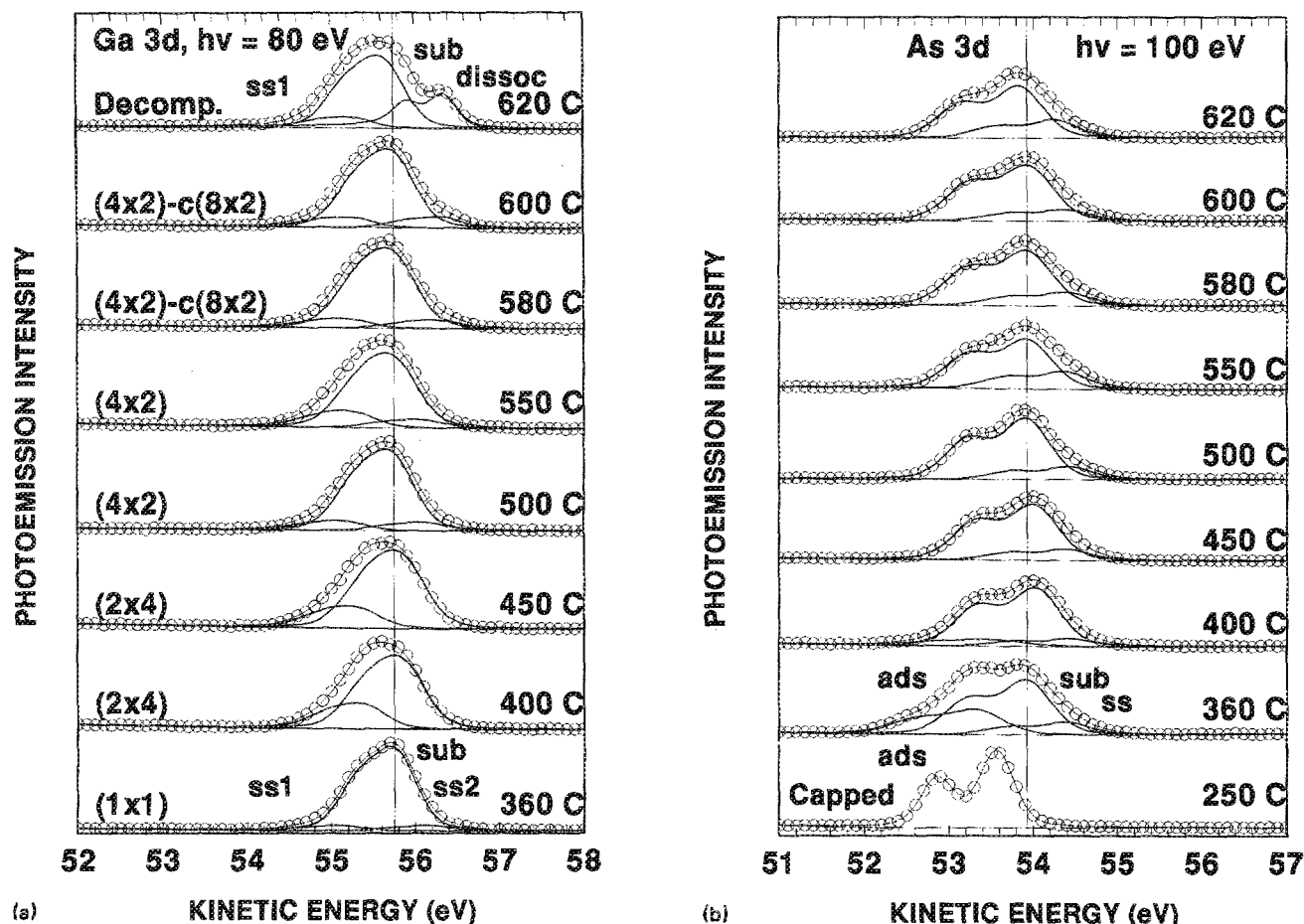


FIG. 1. Surface-sensitive Ga 3d (a) and As 3d (b) core-level spectra of clean GaAs (100) surfaces as a function of desorption temperature and reconstruction. Ga 3d spectra contain two surface-shifted components at the low (ss1) and high (ss2) high kinetic energy from the substrate (sub). As 3d presents a single surface-shifted component (ss). For desorption temperatures below $\sim 450^\circ\text{C}$, adsorbed As produces a spectral component (ads) at the low kinetic energy side of the spectrum.

out using 22 eV incident photon energy and involved measurement of the full EDC width, i.e., the energy separation between the emission from the valence band edge and the onset of the secondary electron emission. The ion gauge was left off, and the sample was biased -7 V relative to both the analyzer and the vacuum chamber during these experiments. This procedure resulted in minimizing the number of stray electrons which could otherwise affect the low energy region of the secondary electron spectra.¹² Low-energy CL spectra from cooled ($\sim 180\text{ K}$) GaAs (100) surfaces and interfaces were assessed in an ultrahigh vacuum (UHV) spectrometer described in detail elsewhere.¹³

The n -type (Si-doped to $7 \times 10^{16}\text{ cm}^{-3}$) GaAs (100) samples were grown by MBE on top of the chemically etched GaAs (100) substrates supplied by Sumitomo Electric. All specimens were capped with relatively thick ($> 1000\text{ \AA}$) As protective coating before removal from the MBE chamber, shipped under vacuum, and then stored in a dry N_2 environment. Pristine surfaces were obtained in cryo pump-equipped analytical chambers by *in situ* thermal desorption of the As coating. The desorption was always carried out in several steps with increasing final temperatures. Each cycle consisted of a nearly linear

temperature ramp ($\sim 5\text{--}10^\circ\text{C/s}$), followed by quenching to the measurement temperature. We evaluated the surfaces after each desorption by SXPS and low-energy electron diffraction (LEED) in terms of surface chemistry, band bending, and surface ordering. To isolate possible effects of the electron beam on these surfaces, separate runs were carried out without using LEED. No significant differences in the E_F position could be discerned between these runs. CLS measurements were preceded by the determination of the starting surface reconstruction and the Auger electron spectroscopy (AES) verification of surface cleanliness and composition.

III. RESULTS AND DISCUSSION

A. Surface reconstruction, chemistry, and band bending

In Fig. 1(a), we show representative Ga 3d spectra for GaAs (100) clean surfaces as a function of As desorption temperature. The spectra were taken at 80 eV incident photon energy, with an estimated escape depth of $\sim 5\text{ \AA}$.¹⁴ These spectra were normalized to the same height and decomposed into several spin-orbit doublets, each reflecting a distinct local environment of Ga atoms in the sub-

strate and at the vacuum interface. Line shape decomposition of these spectra indicates the presence of the substrate Ga 3*d* component (sub) as well as of the two surface-shifted components ss1 and ss2 at the higher and lower binding energy side of the substrate feature, respectively. Each of the components is represented by a Voigt function^{11,14} with the Lorentzian width held constant at 155 meV and the Gaussian width allowed to vary as a fitting parameter. Best fitting consistency was accomplished when the Gaussian widths of the substrate and surface-shifted components were maintained equal.^{7,15} Thus determined Gaussian widths vary between 480 and 580 meV, lower linewidth typically corresponding to surfaces with sharp and well-defined LEED patterns. Relative binding energies and intensities of the surface-shifted components exhibit systematic variations with annealing temperature; the relative kinetic energy of the ss1 feature increases from -0.62 ± 0.02 eV for the (1×1) surface obtained by a 360 °C desorption, to -0.54 ± 0.02 eV for the (4×2)-c(8×2) surfaces obtained in the 500–580 °C temperature range. Correspondingly, the ss2 relative kinetic energy changes from 0.45 ± 0.02 to 0.40 ± 0.02 eV between those surface reconstructions.¹⁶

Relative intensities of the surface-shifted components also change significantly with desorption temperature; the ss2 component is virtually absent at the As-terminated (2×4) surfaces, in contrast with the increased contribution of the ss1 feature at the same surface. For temperatures between ~500 and 600 °C, corresponding to the more Ga-rich (4×2)-c(8×2) surfaces, each component contributes ~9%–11% of the total Ga 3*d* emission. Finally, at temperatures beyond ~600 °C, at the onset of surface decomposition we observe a new component at the high kinetic energy side of the spectrum (0.71 ± 0.02 eV relative to the substrate) which overlaps with the ss2 component. This component exhibits a reduced Gaussian width of ~280 meV (relative to 510 meV for the substrate and ss1 components) and a characteristic metallic line shape asymmetry ($\alpha = 0.09 \pm 0.01$).¹⁶ This component can thus be associated with Ga droplets which are known to form at thermally decomposed surfaces.⁷

Figure 1(b) shows the evolution of surface-sensitive As 3*d* core-level emission as the As cap is thermally desorbed from the surface. The 250 °C desorption removes the top-most oxidized portion of the As coating and produces a well-resolved single-component As 3*d* core-level characteristic of elemental As film atop the GaAs (100) substrate. The 360 °C desorption results in a (1×1) surface whose As 3*d* emission shows a substrate contribution (sub) and a surface-shifted (ss) component at its high kinetic energy side (0.47 ± 0.02 eV relative shift). In addition, the (1×1) surface spectrum contains a third broad feature (ads) at its low kinetic energy end. This feature arises from adsorbed excess As on the surface, although comparison with the 250 °C spectrum reveals that it is significantly broader and shifted to lower kinetic energy relative to the "bulk" As film on the same surface. The broadening is likely due to the inequivalent bonding sites of adsorbed As atoms at the surface. The kinetic energy shift may be due to the differ-

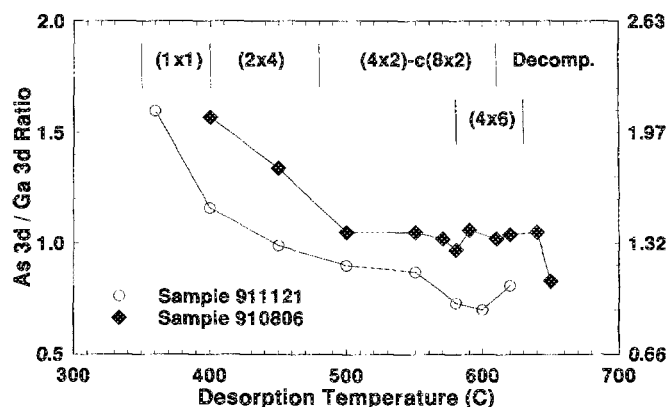


FIG. 2. Total emission intensity ratios between the As 3*d* and Ga 3*d* core levels assessed at 100 and 80 eV, respectively. The scale on the right-hand side is corrected for the relative photoemission cross sections of the two core levels, adopted from Ref. 22. The top of the figure shows typical temperature ranges of our surface reconstructions.

ence in the As local bonding and/or change in surface band bending.^{18–21}

As the desorption temperature is increased above ~400 °C, the adsorbed component contribution is removed from the As 3*d* spectra. The surface-shifted component remains present throughout this temperature range and becomes more prominent as the surface As-content is reduced. Average relative kinetic energy shifts and total intensity contributions of this component are 0.40 ± 0.02 eV and ~13% for the (2×4), and 0.47 ± 0.02 eV and ~22% for the (4×2) surface reconstruction, respectively. Furthermore, we observed pronounced variations in the Gaussian width of the As 3*d* line shape with desorption temperature, in agreement with the similar changes in the Ga 3*d* spectra. The linewidth reduction correlates well with the sharpness of LEED pattern. This suggests that the core level broadening can be associated with the presence of coexisting patches with different surface geometries. Further evidence and possible causes of such surface inhomogeneities will be discussed later in this article.

In Fig. 2, we show the ratio of the As 3*d* and Ga 3*d* total emission intensities measured at 100 and 80 eV photon energies, respectively. The two sets of data points were obtained at samples prepared and studied several months apart and show similar trends with the desorption temperature; the As to Ga ratio starts at ~1.6 for the (1×1) reconstruction, decreases gradually throughout the (2×4) reconstruction temperature range, and stabilizes between 0.8 and 1.0 throughout most of the high temperature range of the (4×2)-c(8×2) reconstruction. For desorption temperatures beyond ~580 °C, this ratio is more difficult to predict because of the possibility of As readsorption and/or outdiffusion from the substrate to the free surface.²³ A significant increase in the As background pressure during these desorptions suggests that both of these processes may be taking place at the onset of surface decomposition. Moreover, when the As partial pressure remained high ($> 1 \times 10^{-9}$ Torr) even between such desorptions, we observed the (4×6) LEED pattern instead of the expected

$c(8 \times 2)$ reconstruction (see Fig. 2, top). These subtle variations provide an indication of the very complex relationship between desorption temperature, surface reconstruction, and chemical composition of decapped MBE-GaAs (100) surfaces.^{7,9,18-21}

The valence band (VB) photoemission spectra (not shown) undergo subtle but important changes with desorption temperature and surface reconstruction, especially in the energy range ~ 1 eV below the valence band maximum (E_v).^{18,19,24} These changes are caused by the presence of surface states for As-rich surfaces,¹⁸ and the presence of metallic states for nearly decomposed As-deficient surfaces. The same VB edge changes can present difficulties when the VB edge extrapolation is used to determine E_F position at GaAs (100) clean surfaces. We attempted to eliminate this source of measurement error by selecting a set of "optimal" VBs obtained from the $c(8 \times 2)$ surfaces and using them to establish the reference ($E_F - E_v$) value of 0.62 ± 0.05 eV. Then we followed rigid shifts in the substrate component of the As 3d and Ga 3d core-level spectra to extract processing-induced changes in band bending relative to these surfaces. Using this method we determined ($E_F - E_v$) of 0.62 ± 0.05 eV for desorption temperatures $500^\circ\text{C} < T < 620^\circ\text{C}$ and the $(4 \times 2)-c(8 \times 2)$ reconstruction, and 0.52 ± 0.05 eV for the more As-rich (2×4) reconstructions produced by 400 and 450°C desorptions. For temperatures beyond $\sim 620^\circ\text{C}$ E_F tends to move closer to the VB maximum, likely due to "pinning" by states produced by surface decomposition. These values of E_F stabilization energy and its relative insensitivity to surface reconstruction are in excellent agreement with other recent measurements on decapped GaAs (100) surfaces.^{7,24}

B. Work function dependence on surface reconstruction

In contrast to the relative insensitivity of the E_F position to surface reconstruction, we provide evidence for large variations in both the surface ionization potential (I) and the work function (Φ) with surface ordering. The surface ionization potential and work function may be determined from photoemission spectra using the following relationship:

$$\Phi = I - (E_F - E_v) = h\nu - \Delta\text{EDC} - (E_F - E_v), \quad (1)$$

where ΔEDC designates the full EDC width of the photoexcited spectrum and $h\nu$ designates the incident photon energy. Hence, a narrow EDC corresponds to a high work function and vice versa. Possible sources of error in SXPS photoemission measurement of work function then include error in the photon energy due to monochromator calibration and errors due to the secondary electron onset, VB edge, and equilibrium E_F determination using a metal reference.¹⁰ Neglecting the first contribution (which also has no bearing on the relative changes in Φ between surface reconstructions), we estimate the overall error in our results to be ~ 100 meV.

Figure 3 displays the measured values of Φ as a function of surface desorption temperature and reconstruction. Filled symbols represent measurements based on the

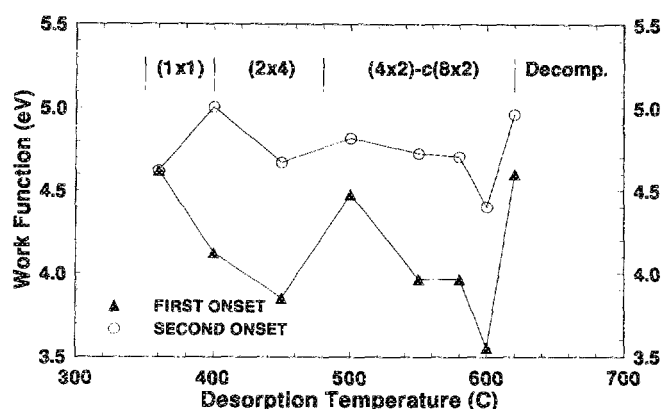


FIG. 3. GaAs (100) surface work function as function of desorption temperature and corresponding surface reconstruction (solid triangles). The contribution of the second emission onsets in Fig. 4 (open circles) reduces the average work function variation between different surface reconstructions.

"first" (low kinetic energy) onset in the secondary electron emission spectra shown in Fig. 4. Empty symbols represent measurements based on the position of a shoulder on the leading edge of some of these spectra, which we will refer to as the "second" (higher kinetic energy) onset in the secondary electron spectra. This second onset appears consistently ~ 0.8 eV relative to the first one for the $c(8 \times 2)$ structure, but both the energy spacing and relative prominence of these onsets change between surface reconstructions. We speculate that these onsets originate from two types of surface domains with distinct values of the surface ionization potential, conceivably those corresponding to the As-dimer and Ga-dimer stabilized surface

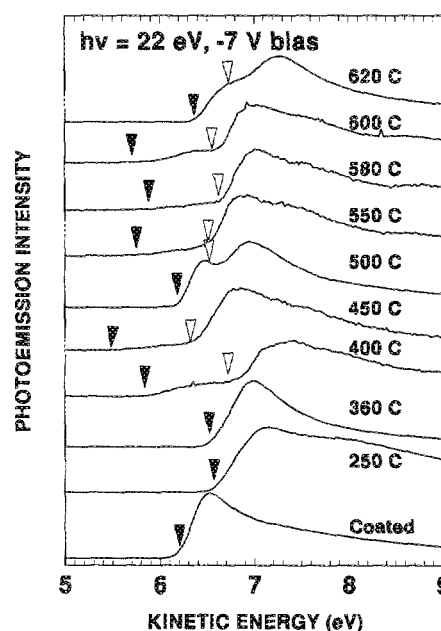


FIG. 4. Secondary electron emission onset at $h\nu = 22$ eV and sample bias of -7 eV relative to the ground. Filled arrows indicate the estimated position of the first and empty arrows of the second onset.

reconstructions.¹⁰ Although a relative measure of the concentration of such domains can be in principle derived from the EDC slopes corresponding to each onset, such measurements are beyond the scope and precision of our experiments.¹⁰ Significantly, the presence of surface inhomogeneities is also evidenced in the broadening of the As 3*d* and Ga 3*d* linewidths for the same transition temperatures.

The work function variations in Fig. 3 (filled symbols) follow the same general trend reported for both decapped MBE-grown^{21,25} and *in situ* prepared GaAs (100) surfaces.^{12,23,26} The work function decreases throughout the (1×1) reconstruction temperature range, reaches a local minimum of 3.85 eV at ~450 °C, and then rises abruptly to a maximum value of ~4.5 eV at 500 °C. For desorption temperatures above 500 °C, the work function decreases to its absolute minimum of ~3.55 eV at 600 °C and finally reaches its measured absolute maximum of ~4.6 eV upon the 620 °C desorption. The maximum value of the work function after the 500 °C desorption appears lower than its values at either end of the desorption temperature range, which differs from the results of Massies *et al.*²⁶ and from the recently obtained results by other research teams.^{21,25} This discrepancy may be due to the fact that we used larger temperature increments and possibly missed the absolute maximum in the work function expected to appear for the *c*(2×8) reconstruction.^{12,26} Indeed, in our UHV system excess As is very efficiently removed from the surface by thermal desorptions, and the As-rich reconstructions are thereby inherently unstable. This agrees with our inability to produce either the *c*(4×4) or the *c*(2×8) LEED patterns commonly observed in MBE-growth systems.²³ Detailed comparison between the results of different groups is hence frustrated by the high sensitivity of "real" surfaces to their preparation conditions. Furthermore, measurement techniques can also introduce significant differences between the surface work function measured by different groups.²⁷ For example, the amplitude of work function variation is ~1.1 eV for our surfaces, which is larger than 0.3–0.8 eV reported by other groups.^{12,21,25,26} This discrepancy may be the result of an averaging of the surface work function by Kelvin probe and retarding beam techniques. Indeed, taking a weighted average of the energies corresponding to both first and second onsets in Fig. 3, one can obtain close consistency between ours and Kelvin probe work function measurements.^{25,26}

Since the E_F position changes by ≤ 100 meV with structure of these surfaces, it is evident that most of the Φ variation is due to the change in the electron affinity. This change is most pronounced between the As-dimer terminated (2×4) and the Ga-rich *c*(8×2) reconstruction and hence points to the central role of the surface dipole in the ionization potential variations.^{10,12,26} Furthermore, the dramatic ~0.9 eV change in Φ over the 500–600 °C desorption temperature range suggests that even for a specific (4×2)-*c*(8×2) LEED pattern, the surface may contain inhomogeneities providing for gradual changes in work function between distinct surface reconstructions.

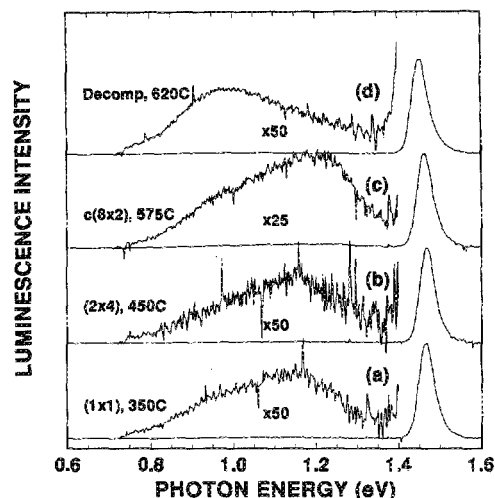


FIG. 5. Surface-sensitive 1 keV CL spectra from GaAs (100) surfaces show subtle changes in energies and intensities of DL features between different clean surface reconstructions.

C. CL measurements of DL

Figure 5 shows surface-sensitive 1 keV CL spectra obtained for four commonly observed surface reconstructions of decapped GaAs (100) surfaces. The DL emission extends between the 0.8 and 1.3 eV photon energy and is relatively weak compared to the near-band gap (NBG) transition at 1.47 eV. Comparison between CL spectra excited with 1, 1.5, and 2 keV incident electron energies reveals a relative enhancement of DL emission with decreasing electron energy, indicative of its near-surface origin.^{6,28} The DL features show subtle changes in energy and intensity between the (1×1), (2×4), and (4×2)-*c*(8×2) surface structures. They indicate a small emission enhancement in the 0.8–1.1 eV range for the most As-rich (1×1) surface, which disappears for the (2×4) and (4×2)-*c*(8×2) surface reconstructions. Finally, incipient surface decomposition at 620 °C strongly enhances the emission band centered at ~0.95 eV, while reducing the emission in the 1.2–1.3 eV range relative to the (4×2)-*c*(8×2) surface.

These subtle but significant differences in the reconstruction-dependent DL emission correlate well with the Fermi-level position at these surfaces. Relative stability of the E_F position over the temperature range corresponding to the (2×4) and (4×2)-*c*(8×2) surface structures is in agreement with the observed lack of major DL changes between these reconstructions. Alternatively, the additional bandgap features introduced at both the As-rich and the Ga-rich end of the surface composition range correlate well with the E_F movement toward the valence band maximum observed under similar conditions.²⁴

IV. CONCLUSIONS

This work demonstrates unequivocally that chemical, structural, and electronic properties of decapped GaAs (100) surfaces vary systematically with surface reconstruction and desorption temperature. Surface reconstruction is found to depend sensitively on both the desorption temper-

ature and processing conditions, among which the As background pressure seems particularly important. Synchrotron radiation photoemission measurements indicate gradual and systematic changes in core level and valence band emission with desorption temperature and surface reconstruction. Surface chemical composition and work function vary predictably with desorption temperature and surface reconstruction. Core-level features and spectral structure at the onset of secondary electron emission indicate the presence in varying degrees of surface inhomogeneities throughout the range of desorption temperatures. The chemical and electronic complexity of decapped GaAs (100) surfaces clearly indicates that a multitechnique approach, involving core level and valence band photoemission, band gap luminescence, and LEED spectroscopy, is necessary for their unique characterization.

ACKNOWLEDGMENTS

The authors would like to thank Professor A. Kahn for useful discussions and for his experimental results prior to their publication. The authors also thank D. F. Rioux for his assistance in the experimental work. Photoemission measurements were performed at the NSF-supported Synchrotron Radiation Center of the University of Wisconsin-Madison. Assistance of the SRC staff is gratefully acknowledged. This work was in part supported by the Office of Naval Research Contract No. N00014-91-C-0037.

¹See, for example, E. H. Rhoderick and R. H. Williams in *Metal-Semiconductor Contacts*, 2nd ed. (Clarendon, Oxford, 1988), and references therein.

²L. J. Brillson, *Surf. Sci. Rep.* **2**, 123 (1982).

³J. H. Weaver, in *A New Era in Materials Science*, edited by J. R. Chelikowsky and A. Franciosi (Springer, Berlin, in press), Chap. 7.

⁴C. J. Palmström, T. L. Cheeks, H. L. Gilchrist, J. G. Zhu, C. B. Carter, and R. E. Nahory, Materials Research Society Extended Abstract, Materials Research Society, 1990 (unpublished), Abstract EA-21; see also T. Sands, C. J. Palmström, J. P. Harbison, V. G. Keramidas, N. Tabatabaie, T. L. Cheeks, R. Ramesh, and Y. Silberberg, *Mater. Sci. Rep.* **5**, 99 (1990).

⁵R. E. Viturro, S. Chang, J. L. Shaw, C. Mailhot, L. J. Brillson, A.

Terassi, Y. Hwu, G. Margaritondo, P. D. Kirchner, and J. M. Woodall, *J. Vac. Sci. Technol. B* **7**, 1007 (1989).

⁶I. M. Vitomirov, A. D. Raisanen, A. C. Finnefrock, R. E. Viturro, L. J. Brillson, P. D. Kirchner, G. D. Pettit, and J. M. Woodall, (unpublished).

⁷G. Le Lay, D. Mao, A. Khan, Y. Hwu, and G. Margaritondo, *Phys. Rev. B* **43**, 14301 (1991).

⁸R. E. Viturro, J. L. Shaw, L. J. Brillson, J. M. Woodall, P. D. Kirchner, G. D. Pettit, and S. L. Wright, *J. Vac. Sci. Technol. B* **6**, 1397 (1988).

⁹R. Z. Bachrach, R. S. Bauer, P. Chiaradia, and G. V. Hansson, *J. Vac. Sci. Technol.* **19**, 335 (1981).

¹⁰W. Ranke, *Phys. Rev. B* **27**, 7807 (1983), and references therein.

¹¹J. J. Joyce, M. Del Giudice, and J. H. Weaver, *J. Electron Spectrosc. Relat. Phenom.* **49**, 31 (1989).

¹²K. Hirose, E. Foxman, T. Noguchi, and M. Uda, *Phys. Rev. B* **41**, 6076 (1990), and references therein.

¹³L. J. Brillson, R. E. Viturro, J. L. Shaw, and H. W. Richter, *J. Vac. Sci. Technol. A* **6**, 1437 (1988).

¹⁴M. C. Schabel, I. M. Vitomirov, G. D. Waddill, and J. H. Weaver, *J. Electron Spectrosc. Relat. Phenom.* **56**, 211 (1991).

¹⁵C. J. Spindt, M. Yamada, P. L. Meissner, K. E. Miyano, A. Herrera, A. J. Arko, and W. E. Spicer, *J. Vac. Sci. Technol. B* **9**, 2091 (1991).

¹⁶Relative binding energies and emission intensities of the surface-shifted components are a sensitive function of surface processing, e.g., of the As presence in the chamber and details of thermal desorptions; whereas the ss1 and ss2 components for the Ga 3d spectra shown in Fig. 1 are offset by 0.55 and -0.40 eV relative to the substrate emission, measurements in a different run produced shifts of 0.34 ± 0.02 eV and -0.33 ± 0.02 eV for the same, $(4 \times 2)-(8 \times 2)$, surface reconstruction, in closer agreement with Refs. 7 and 15.

¹⁷S. Doniach and M. Sunjic, *J. Phys. C* **3**, 285 (1970).

¹⁸J. F. van der Veen, P. K. Larsen, J. H. Neave, and B. A. Joyce, *Solid State Commun.* **49**, 659 (1984).

¹⁹J. F. van der Veen, L. Smit, P. K. Larsen, and J. H. Neave, *Physica B* **117 & 118**, 822 (1983).

²⁰R. Ludeke, T.-C. Chiang, and D. E. Eastman, *Physica B* **117 & 118**, 819 (1983).

²¹R. Duszak, C. J. Palmström, C. J. Sandroff, Y.-N. Yang, and J. H. Weaver, *J. Vac. Sci. Technol. B* **10**, 1891 (1992).

²²J. J. Yeh and I. Lindau, *Atomic Nucl. Data Tables* **32**, 1 (1985).

²³C. J. Palmström (private communication).

²⁴I. M. Vitomirov, A. D. Raisanen, L. J. Brillson, P. D. Kirchner, G. D. Pettit, and J. M. Woodall (unpublished).

²⁵W. Chen, D. Mao, M. Dumas, and A. Khan, *J. Vac. Sci. Technol. B* **10**, 1886 (1992).

²⁶J. Massies, P. Devoldere, and N. T. Linh, *J. Vac. Sci. Technol.* **16**, 1244 (1979).

²⁷L. Däweritz, *Surf. Sci.* **160**, 171 (1985).

²⁸L. J. Brillson and R. E. Viturro, *Scan. Electron Microsc.* **2**, 789 (1988).